https://doi.org/10.5194/egusphere-2025-5093
Preprint. Discussion started: 28 October 2025

Temperature–RH Dependent Viscosity of Organic Aerosols from 273 to 303 K: Implications for Global N_2O_5 Uptake

Atta Ullah[1], Ying Li[2], Mijung Song[1,3]

[1]Department of Earth and Environmental Sciences, and Earth Environmental System Research Center, Jeonbuk National University, Jeollabuk-do Jeonju-si 54896, Republic of Korea; [2] Key Laboratory of Industrial Ecology and Environmental Engineering (Ministry of Education), School of Environmental Science and Technology, Dalian University of Technology, Dalian 116024, China; [3]Department of Environment and Energy, Jeonbuk National University, Jeollabuk-do Jeonju-si 54896, Republic of Korea

Correspondence to: Mijung Song (Mijung.Song@jbnu.ac.kr)

https://doi.org/10.5194/egusphere-2025-5093
Preprint. Discussion started: 28 October 2025

Abstract

Organic aerosol (OA) viscosity and phase state govern multiphase diffusion and reactivity, yet systematic constraints across tropospheric temperature (T)–relative humidity (RH) space remain limited. We measured the viscosity of sucrose–H_2O droplets (OA surrogate) over 273–303 K and ~20–90% RH using bead-mobility and poke-and-flow methods, spanned ~9 orders of magnitude. A Vogel–Fulcher–Tammann fit with experimentally derived fragility (D_f = 13) extended the parameterization to 230–310 K and 0–100% RH. When coupled with zonal-mean tropospheric T–RH fields (2020–2024), the parameterization yielded global distributions of viscosity and organic-phase mixing time ($\tau_{mix,org}$) for 200-nm particles: liquid states prevailed below ~2 km, semisolid regimes occupied ~2–9 km (latitude dependent), and near-glassy conditions emerged above ~9 km; $\tau_{mix,org}$ was <1 h in the boundary layer but frequently exceeded 1 h aloft. Calculations indicated the N_2O_5 uptake coefficient was generally $\geq 10^{-2}$ for liquid particles in the boundary layer, decreased by ~1–2 orders above ~2–4 km as bulk diffusion became rate-limiting; with surface hydrolysis, N_2O_5 uptake coefficient leveled near ~$10^{-3.5}$ aloft, and without it can drop to 10^{-5}–10^{-6} at viscosity $\gtrsim 10^9$ Pa·s. These results highlight the need for temperature-sensitive viscosity in next-generation air-quality and climate models.

KEYWORDS. Viscosity, Phase state, Temperature, Relative humidity, Organic aerosol, Mixing time, N_2O_5 uptake

https://doi.org/10.5194/egusphere-2025-5093
Preprint. Discussion started: 28 October 2025

1 Introduction

Organic aerosols (OAs), including both primary (POA) and secondary organic aerosol (SOA), are ubiquitous in the Earth's atmosphere. These aerosols play vital roles in climate, air quality, and human health through their interactions with solar radiation, cloud microphysics, and heterogeneous atmospheric chemistry (Pandis et al., 1992; Pöschl, 2005). In the troposphere, OA is frequently exposed to a wide range of relative humidity (RH) and temperature, conditions that drive phase transitions that profoundly modify its physicochemical properties.

Depending on chemical composition, RH, and temperature, OA can exist in liquid, semi-solid, or solid (or glassy) states (Koop et al., 2011; Reid et al., 2018). Dynamic viscosity serves as a useful parameter for classifying these states: viscosity < 10^2 Pa·s corresponds to a liquid phase, $10^2 \leq$ viscosity $\leq 10^{12}$ Pa·s to a semi-solid phase, and viscosity > 10^{12} Pa·s a glassy phase (Koop et al., 2011; Reid et al., 2018). Accurate determination of aerosol viscosity and phase state is critical for predicting heterogeneous reaction kinetics (Zhou et al., 2013; Marshall et al., 2018), particle size distributions (Shiraiwa and Seinfeld, 2012; Shiraiwa et al., 2013; Zaveri et al., 2018; Song et al., 2022), and ice nucleation (Knopf et al., 2018; Ladino et al., 2014; Lienhard et al., 2015). Highly viscous SOA matrices impede molecular diffusion, suppress oxidant uptake, and finally can alter SOA yields (Abbatt et al., 2012; Gržinić et al., 2015a; Kuwata and Martin, 2012).

Over the past two decades, laboratory and modeling studies have established RH as a primary control on OA viscosity at near-room temperature, transitioning from liquid to semi-solid or glassy as RH decreases (Song et al., 2015a; Song et al., 2016a; Song et al., 2019a; Song et al., 2016b; Song et al., 2021b; Gerrebos et al., 2024; Gregson et al., 2023; Kiland et al., 2023; Nikkho et al., 2024; Grayson et al., 2016; Grayson et al., 2017; Saukko et al., 2012). The role of chemical compositions on OA viscosities has also been widely explored, showing that parameters such as oxygen-to-carbon ratio, molar mass, functional group and volatility diversity can significantly affect the phase state and viscosity of OA (Derieux et al., 2018; Grayson et al., 2017; Rothfuss and Petters, 2017a; Li et al., 2020; Champion et al., 2019; Shiraiwa et al., 2017). However, despite substantial progress on RH- and

https://doi.org/10.5194/egusphere-2025-5093
Preprint. Discussion started: 28 October 2025

composition-dependence, the explicit role of temperature across the tropospheric range (230 – 310 K) remains poorly constrained. While there have been modeling efforts to predict viscosity changes with temperature using parameterizations such as the fragility parameter or Vogel-Fulcher-Tammann (VFT) frameworks (Kiland et al., 2023; Rothfuss and Petters, 2017b; Gerrebos et al., 2024; Kasparoglu et al., 2021), experimental studies that directly probe temperature-dependent viscosity remain scarce.

This gap in temperature-dependent viscosity data has significant implications for heterogeneous chemistry. For instance, high viscosity can suppress reactive gas uptake by several orders of magnitude (Shiraiwa et al., 2011; Marshall et al., 2016). Modeling and field observations indicated that viscous organic shells can reduce the N_2O_5 uptake coefficient by 1–3 orders of magnitude (Song et al., 2025a), while liquefaction can restore reactivity by a factor of 10 to 100 (Gržinić et al., 2015a; Hallquist et al., 2003). Therefore, improving our understanding of OA viscosity depending on atmospheric condition including temperature variations is critical for accurately representing heterogeneous processes in atmospheric models.

To address this knowledge gap, we conducted a systematic experimental investigation of OA viscosity under tropospherically relevant temperature and RH conditions, utilizing sucrose as a well-characterized OA model compound (Power et al., 2013; Zobrist et al., 2011; Bateman et al., 2014; Kiland et al., 2019). Viscosity was measured at 273, 283, 293, and 303 K and 20 – 90% RH using bead-mobility and poke-and-flow techniques. The measured viscosity data were parameterized to construct a T-RH phase diagram for sucrose-H_2O droplets. Based on parameterized viscosity, we analyzed global zonal-mean profiles of viscosity and the corresponding mixing times of organic molecules ($\tau_{mix,org}$) within 200 nm sucrose particles. Finally, we predicted heterogeneous N_2O_5 uptake coefficient across tropospheric T–RH conditions using the viscosity fields in a mechanistic framework that accounts for bulk diffusion and surface hydrolysis.

https://doi.org/10.5194/egusphere-2025-5093
Preprint. Discussion started: 28 October 2025

2 Experimental and Methods

2.1 Materials and aerosol generation

Sucrose (99.5% purity, Sigma-Aldrich) was dissolved in high-purity water (18 MΩ·cm, Merck Millipore Synergy, Germany) to prepare approximately 10 wt.% aqueous solutions. In all experiments, sucrose droplets were generated by nebulizing an aqueous solution with a low-internal-volume glass nebulizer (Meinhard, USA) and depositing them onto a hydrophobic substrate (Hampton Research, Canada). Using the droplets, we systematically determined their viscosity across four temperatures (273, 283, 293, and 303 K) and a wide range of RH conditions (20 – 90 %) via bead-mobility, and poke-and-flow.

2.2 Viscosity measurements by bead-mobility technique ($\eta \approx 10^{-3}$ - 10^{3} Pa·s)

The bead-mobility technique has been described in detail elsewhere (Renbaum-Wolff et al., 2013a; Jeong et al., 2022; Song et al., 2015a; Renbaum-Wolff et al., 2013c); here, we briefly summarize the procedure as applied in this work. Insoluble melamine beads (~1 µm, Cat. No. 86296, Sigma-Aldrich) were nebulized into sucrose-H_2O droplets deposited on a hydrophobic substrate (diameter: ~40–100 µm) in a flow-cell (TSA12Gi, INSTEC, USA). A total N_2/H_2O gas flow of 1.2 L min^{-1} generated a uniform shear stress on the droplet surfaces at high RH (60 – 90%) and temperature (273 – 303 K).

Prior to each measurement, the droplets were equilibrated at the target RH and temperature for sufficient time to ensure thermodynamic conditioning. At each temperature, RH was systematically reduced every ~5 % from ~90 to ~60 %, with the exact RH steps varying between experiments. During the experiment, the bead motion in a droplet was recorded with an optical microscope (Olympus CKX53 with 40 × objective, Japan) and CCD camera (Hamamatsu C11440-42U30, Japan). The bead velocities were then converted to viscosity using a calibration curve (Fig. S1). Figure S2 shows representative bead movements within sucrose droplets at different temperatures. The corresponding mean bead speeds as a function of temperature and RH are presented in Fig. S3a, and the

https://doi.org/10.5194/egusphere-2025-5093
Preprint. Discussion started: 28 October 2025

derived viscosities obtained using the calibration curve (Fig. S1) are shown in Fig. S3b. When the bead movements were too slow to measure, the poke-and-flow technique was applied.

2.3 Viscosity measurements by poke-and-flow (η > ~10^3 Pa·s)

The poke-and-flow technique is widely used to determine the viscosity of highly viscous single droplets (Grayson et al., 2015; Gerrebos et al., 2024; Song et al., 2015b; Renbaum-Wolff et al., 2013c). In this study, sucrose-H_2O droplets with diameters ranging from ~20 to ~40 µm on a hydrophobic glass substrate were conditioned in the flow-cell. At each temperature (273, 283, 293, and 303 K), RH was systematically reduced from approximately 60% to lower levels in discrete steps (typically ~5%), and the poke-and-flow method was applied until either viscous flow or particle fracture was observed. The required conditioning time of each droplet for thermodynamic equilibrium was determined for each RH-T setting and are described in Section S1 and Table S1. After equilibration, each droplet was poked using a fine needle (Jung Rim Medical Industrial, South Korea), mounted on a micromanipulator (Narishige, model MO-152, Japan). The morphological evolution of the droplets before, during, and after poking was monitored via optical microscopy (Olympus CKX53 with a 40× objective, Japan) and captured using a CCD camera (Hamamatsu, C11440-42U30, Japan).

The experimental flow time, $\tau_{exp,flow}$, was defined as the time required for the diameter of the central cavity to reduce to 50% of its value immediately after poking. Figure S4 presents representative optical images showing the morphological evolution of a sucrose–H_2O droplet at ~50% RH for 273 – 303 K during the experiment. Averaged $\tau_{exp,flow}$, reflecting temperature and RH dependence are summarized in Fig. S5a. These values of sucrose-H_2O droplets were then converted to the viscosity using the equation proposed by Sellier et al. (2015) resulting viscosities shown in Fig. S5b. At lower RH, brittle cracking without relaxation after poking was observed as shown in Fig. S6. When restorative flow was not detected after more than 2 h, we assigned the viscosity as ≥ 1×10^8 Pa·s (Song et al., 2021b; Jeong et al., 2022; Song et al., 2019b; Renbaum-Wolff et al., 2013c; Maclean et al., 2021a).

https://doi.org/10.5194/egusphere-2025-5093
Preprint. Discussion started: 28 October 2025

2.4 Determination of fragility parameter and glassy phase transition

To determine the fragility parameter (D_f), which describes how sensitively viscosity responds to temperature near the glass transition, we fitted our experimental viscosity data—spanning a temperature range of 273 – 303 K and RH ~20 – 90% — to the VFT equation Eq. (1).

$$ln\,\eta(\mathrm{RH},\mathrm{T}) = ln\,\eta_\infty + \frac{D_f T_o(RH)}{T - T_o(RH)} \tag{1}$$

where η(RH, T) is the viscosity at a given RH and temperature, $\eta_\infty = 1 \times 10^{-5}$ Pa·s is the viscosity at infinite temperature,(Angell, 1991) and $T_0(RH)$ is the RH-dependent Vogel temperature, which can be obtained by rearranging Eq. (1):

$$\mathrm{T_o}\,(RH) = \frac{ln\left(\frac{\eta\,(RH,293\mathrm{K})}{\eta_\infty}\right)\,(293K)}{D_f + \ln\left(\frac{\eta\,(RH,293K)}{\eta_\infty}\right)} \tag{2}$$

where $\eta(RH$, 293 K), is the viscosity at 293 K, estimated using a mole-fraction-based Arrhenius mixing rule. Fitting this relation yielded a hygroscopicity parameter k = 0.061 ± 0.0023 (Fig. S7), and full parametrization details are provided in Section S2. Figure S8 shows the resulting best-fit value for D_f as 13 ± 1, which is derived directly from temperature-dependent viscosity measurements. While prior studies often relied on assumed or literature-based D_f values (generally ~10) for various SOA types (Kiland et al., 2023; Maclean et al., 2021b; Gregson et al., 2023; Derieux et al., 2018), this work provides the first experimentally constrained estimate of D_f based on the temperature dependent viscosity data for sucrose-H_2O droplets.

https://doi.org/10.5194/egusphere-2025-5093
Preprint. Discussion started: 28 October 2025

2.5 Simulation of N_2O_5 uptake coefficient

Simulations of the N_2O_5 uptake coefficient are based on the resistor model,(Ammann et al., 2013; Gržinić et al., 2015b) which has been detailed in our previous study (Song et al., 2025b). Principally, N_2O_5 uptake coefficient is calculated considering surface accommodation, surface reaction, transfer from surface to bulk, and the bulk reaction-diffusion resistance. As shown in Eq. (3), the surface accommodation coefficient (α_s) is set to be 1 assuming that surface accommodation is not rate limiting. Γ_s represents the limiting uptake coefficient for the surface reaction, which was estimated to be 2.5 $\times 10^{-4}$ based on previous simulations and observations at low RH conditions (Gržinić et al., 2015b). $1/\Gamma_{sb}$ represents the resistance for surface to bulk transfer, calculated by $1/\Gamma_{sb} = 1/\alpha_b - 1/\alpha_s$, where α_b is set to be 0.035 (Gržinić et al., 2015b; Song et al., 2025b). $1/\Gamma_b$ represents the bulk reaction-diffusion resistance given by Eq. (4).

$$\frac{1}{\gamma_{N_2O_5}} = \frac{1}{\alpha_s} + \frac{1}{\Gamma_s + \left(\frac{1}{\Gamma_{sb}} + \frac{1}{\Gamma_b}\right)^{-1}} \tag{3}$$

$$\frac{1}{\Gamma_b} = \frac{\omega}{4HRT\sqrt{D_{N2O5}k^I}}\left(\coth q - \frac{1}{q}\right)^{-1} \tag{4}$$

Values of the mean thermal velocity of N_2O_5 (ω), the Henry's law constant (H), and the hydrolysis rate (k^I) in Eq. (4) are taken from our previous study (Song et al., 2025b). R is the gas constant. The reacto-diffusive parameter (q) is calculated as r/l, where r is the radius of sucrose particles, assumed to be 100 nm in this study. l is the reacto-diffusive length, defined by $\sqrt{D_{N2O5}/k^I}$, where D_{N2O5} is the diffusivity coefficient of N_2O_5 in OA calculated from the fractional Stokes-Einstein equation as described in Section S1.

https://doi.org/10.5194/egusphere-2025-5093
Preprint. Discussion started: 28 October 2025

3 Results and discussion

3.1 Temperature and RH dependent-viscosities of sucrose-H_2O droplets

Figure 1 illustrates the effect of temperature on the viscosity of sucrose-H_2O droplets across a range of RH. In this study, we systematically investigated viscosity changes at four specific temperatures—273, 283, 293, and 303 K—across a 30 K range and RH values from ~20 to ~90%. The result shows that viscosity of the droplets varied by approximately nine orders of magnitude, suggesting the strong temperature sensitivity modulated by RH. At 293 K, the current result agrees with previous studies (Jeong et al., 2022; Song et al., 2021a; Song et al., 2016a; Song et al., 2015a; Power et al., 2013; Grayson et al., 2015; Renbaum-Wolff et al., 2013b), confirming the robustness of our measurements. At other temperature, however, viscosity data are scare, and thus our study provides the first systematic benchmarks across 273 – 303 K, filling a critical gap in the literature.

As temperature increased from 273 to 303 K, viscosity consistently decreased, with the magnitude of reduction depending on RH. For example, at high RH (~74 – 80 %), viscosity decreased by approximately one order of magnitude—from ~1.2×10^{1} Pa·s at 273 K to ~1.9×10^{0} Pa·s at 303 K, which correspond to a liquid state (Fig. 1). At mid RH (~50%), the temperature increase caused a much larger reduction, from ~2.1×10^{6} Pa·s at 273 K to ~1.4×10^{3} Pa·s at 303 K, indicating a semi-solid state. This behavior was directly observed in optical images during poke-and-flow experiments (Fig. S4), which revealed distinct flow-time contrasts between the temperature ranges.

At lower RH, the droplets exhibited brittle cracking by poking at all temperatures. The cracking RH threshold decreased systematically with increasing temperature: ~38% RH at 273 K, ~33% at 283 K, ~24% at 293 K, and ~18% at 303 K (Fig. S6). Once fracture occurred, no restorative flow was observed for more than two hours, indicating a near- glassy state (viscosity > 1×10^{8} Pa·s) (Song et al., 2021b; Jeong et al., 2022). The viscosity difference associated with a 30 K temperature shift becomes increasingly pronounced at lower RH, highlighting the combined sensitivity of OA phase behavior to both temperature and RH.

https://doi.org/10.5194/egusphere-2025-5093
Preprint. Discussion started: 28 October 2025

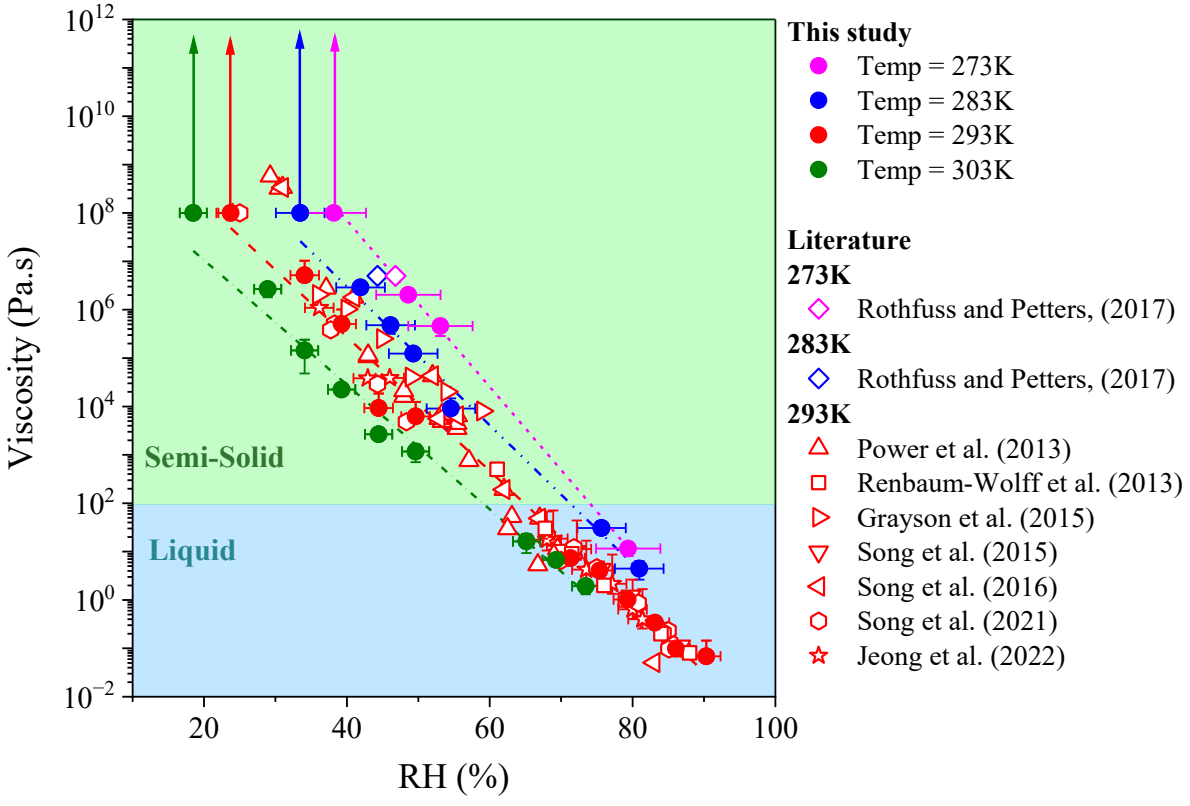

Figure 1: Viscosity data from bead mobility and poke-and-flow experiments at 273 ± 1 K (magenta circles), 283 ± 1 K (blue circles), 293 ± 1 K (red circles) and 303 ± 1 K (green circles) across a RH range of 20 – 90%. The *x*-axis error bars represent the uncertainty in RH from the RH sensor during calibration at each temperature, while the *y*-error bars show the standard deviation in the measured viscosity calculated from 3 – 5 beads across 2 – 5 particles. Dotted lines show linear fit of viscosity versus RH at each temperature, with line colors matching the symbol colors for the corresponding temperatures. Experimental data from previous studies are included for comparison (Power et al., 2013; Rothfuss and Petters, 2017b; Renbaum-Wolff et al., 2013b; Grayson et al., 2015; Song et al., 2015a; Song et al., 2016a; Song et al., 2021a; Jeong et al., 2022).

https://doi.org/10.5194/egusphere-2025-5093
Preprint. Discussion started: 28 October 2025

We then extended the results with the VFT equation to calculate viscosity across a wider range of RH (0 – 100 %) and temperature (230 – 310 K), using the fragility parameter (D_f = 13) directly derived from our experimental measurements. Figure 2 illustrates the resulting RH–temperature phase diagram, in which contour lines (isopleths) of constant viscosity.

The orientation of these isopleths varies systematically with temperature. At low temperatures (T < 240 K, representative of the upper troposphere, ~8 – 12 km), the contours are nearly vertical. This shows that viscosity is extremely sensitive to RH, and even small increases in RH can decrease viscosity by several orders of magnitude. Between 240 and 280 K (typical of the middle troposphere, ~3 – 8 km), the contours display moderate slopes, reflecting the combined influence of both temperature and RH. At higher temperatures (280 – 310 K, representative of the lower troposphere, ~0 – 3 km), the contours show gentler slopes compared to colder conditions.

OAs in the upper troposphere are highly sensitive to RH, whereas those near the surface show reduced RH sensitivity with a relatively greater influence from temperature. Importantly, the phase diagram spans the full 0 – 100% RH space to illustrate potential behavior, yet its interpretation should be considered in light of the actual ranges of RH and temperature observed in the troposphere, which vary regionally and seasonally.

https://doi.org/10.5194/egusphere-2025-5093
Preprint. Discussion started: 28 October 2025

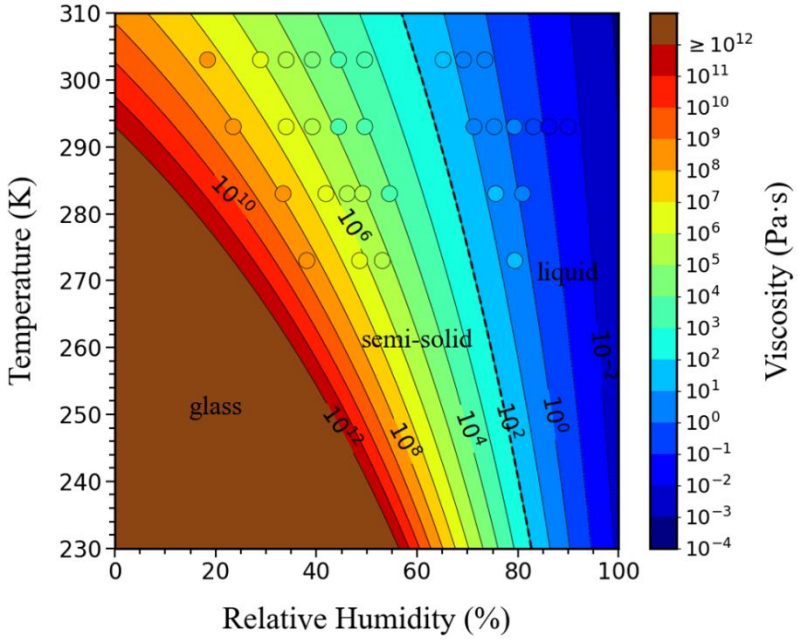

Figure 2: Phase diagram showing viscosity isopleths for sucrose-H_2O droplets as a function of temperature and RH. Viscosity isopleths were computed using the VFT equation, with the D_f obtained from experimental data to VFT equation (Fig. S8). Overlaid circles show the experimental data points for viscosity measured at specific temperature and RH conditions as shown in Fig. 1. The black dash line indicates the transition from liquid to semi-solid of sucrose-H_2O droplet. The brown area represents the temperature and RH conditions where the sucrose-H_2O droplets exhibit a glassy state.

3.2 Viscosity and mixing times of sucrose-H_2O droplets at a range of tropospheric conditions

Building on the phase diagram in Fig. 2, we applied the viscosity parameterization to reanalysis-based RH and temperature fields to evaluate realistic tropospheric conditions. Figure 3 presents the zonal-mean distributions of (a) viscosity and (b) $\tau_{mix,org}$ within 200 nm of sucrose droplets as a function of latitude and altitude, derived from monthly mean ambient RH and temperature from 2020 to 2024 (Fig. S9 and Section S3). $\tau_{mix,org}$ was calculated from the viscosity values using the Stokes–Einstein equation as described in the Section S1 (Eq. S1.5),

https://doi.org/10.5194/egusphere-2025-5093
Preprint. Discussion started: 28 October 2025

representing the time required for organic molecules to equilibrate within a 200 nm droplet and thus indicating the time of internal mixing.

In Fig. 3a, zonal-mean viscosity values of sucrose-H_2O droplets revealed a clear stratification: liquid phase states dominate below ~2 km, semi-solid states exist between ~2 and ~9 km depending on latitude, and glassy states emerge above ~9 km. At high latitudes (> 70 °) in southern hemispheres, liquid phases extended to ~3 – 4 km above the surface (Fig. 3a), higher than in the tropics and northern hemisphere polar region where liquid states are typically confined below ~2 km. This persistence is consistent with the extremely high RH observed in these regions (Fig. S9), which enhances water uptake and plasticization of the organic matrix, thereby suppressing viscosity. Semi-solid regimes also extended to higher altitudes in the polar regions than in the midlatitudes, reflecting the moderating influence of RH against the transition to glassy states. Compared with Shiraiwa et al. (2017) who predicted SOA phase state with a global chemistry climate model (EMAC–ORACLE) using regionally and vertically resolved meteorology, our estimates are derived from zonal-mean tropospheric T–RH fields and a single-component sucrose–H_2O surrogate. Zonal averaging damps low-RH/low-T extremes that promote glassy states, and sucrose is strongly plasticized by water; together these factors tend to diagnose lower Tg/T (i.e., less viscous) than the multi-component SOA fields reported.

Using the viscosity data of sucrose-H_2O droplets and the Stokes–Einstein equation, Fig. 3b shows the calculated $\tau_{mix,org}$ of organic molecules in 200 nm sucrose droplets. Results indicate that the $\tau_{mix,org}$ of sucrose droplets was shorter than 1 hour at all latitudes in the lower troposphere (< ~2 km). Above ~2 – 9 km, $\tau_{mix,org}$ of sucrose droplets frequently exceeded 1 hour in the middle to upper troposphere. This result contrasts with the common assumption in chemical transport models that mixing is always rapid (typically ~1 h), implying that such models likely underestimate kinetic limitations in the troposphere.

https://doi.org/10.5194/egusphere-2025-5093
Preprint. Discussion started: 28 October 2025

Our analysis focuses on sucrose as a proxy system, but real atmospheric aerosols are chemically more complex and often internally mixed with inorganic salts or primary organics. Inorganic components, owing to their hygroscopicity, would generally lower viscosity by enhancing water uptake, thereby shortening $\tau_{mix,org}$ under humid conditions. Further work is therefore required to investigate viscosity and mixing times in multi-component aerosol systems.

https://doi.org/10.5194/egusphere-2025-5093
Preprint. Discussion started: 28 October 2025

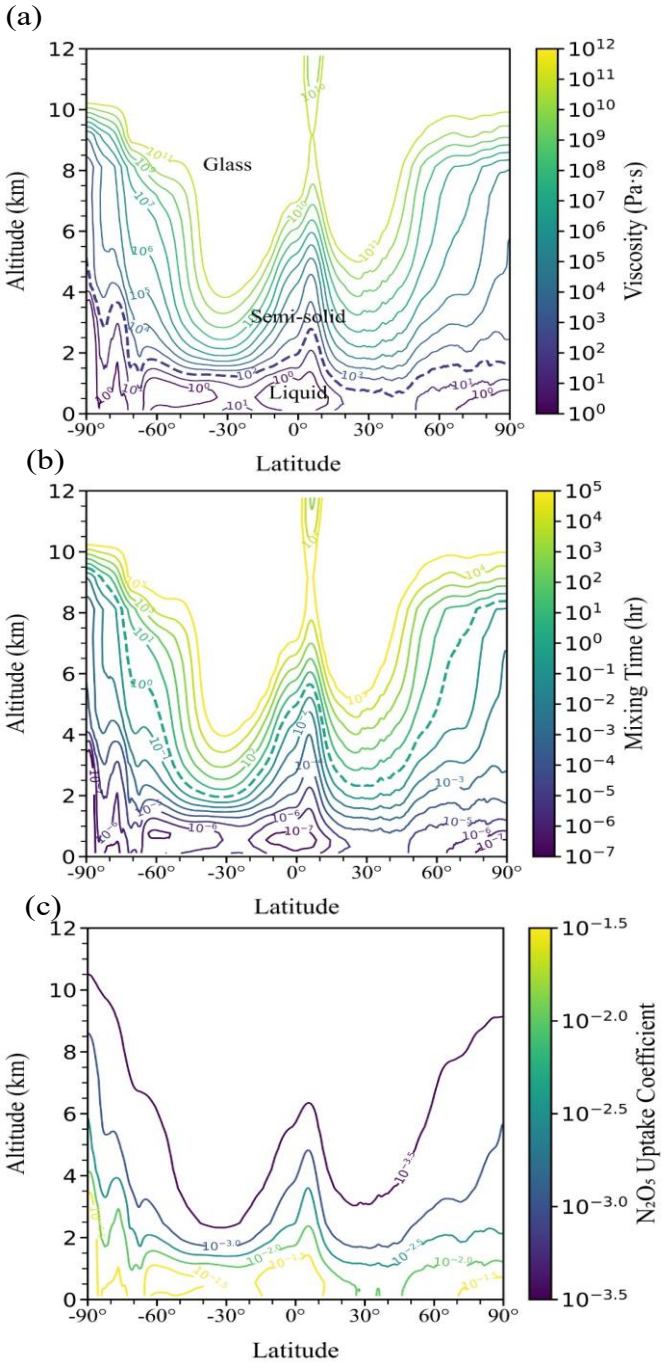

https://doi.org/10.5194/egusphere-2025-5093
Preprint. Discussion started: 28 October 2025

Figure 3: Annual zonal-mean global profiles for (a) viscosity (b) mixing times of organic molecules, and (c) N_2O_5 uptake coefficient in 200 nm sucrose droplets as a function of altitude and latitude based on average annual RH and temperature fields for the years 2020 to 2024, obtained from Copernicus Climate Data Store (https://cds.climate.copernicus.eu/). The purple dashed line in panel (a) shows the viscosity for 10^2 Pa·s. The green dashed line in (b) shows the mixing time of 1 hr. Seasonal variability of the viscosity and mixing times for sucrose-H_2O droplets is shown in Fig. S10.

4 Atmospheric implications

4.1 Global N_2O_5 uptake

Viscosity-induced diffusion limitation has direct consequences for heterogeneous chemistry. For example, highly viscous sucrose matrices suppress the transport of N_2O_5 and water into particle bulk, potentially lowering reactive uptake coefficients by orders of magnitude. Conversely, under warm and humid conditions, liquefaction increases diffusivity, enhancing uptake. Using our parameterized viscosity fields, we estimated that in the midlatitude upper troposphere, suppressed uptake could extend over several shorts of the year, particularly in winter. This aligns with recent field observations showing reduced N_2O_5 loss rates in cold conditions (Zhang et al., 2025; Wagner et al., 2013). While these results are presented here as a case study, they illustrate the strong temperature dependence of multiphase reactivity.

For liquid particles, the N_2O_5 uptake coefficient of is generally higher than ~10^{-2}, and is most prevalent in the atmospheric boundary layer. When altitude exceeds ~ 2 – 4 km depending on latitudes, N_2O_5 uptake coefficient decreases by 1 – 2 orders of magnitude, implying that the N_2O_5 uptake rates of can be limited by slow bulk diffusion within viscous particles, which may lead to decreased concentrations of particulate nitrates or increased gas-phase NO_3 (You et al., 2012). On highly viscous or glassy particles, surface hydrolysis can dominate the uptake. As shown in Fig. 3c, N_2O_5 uptake coefficient is leveled on ~$10^{-3.5}$ when altitudes continue to increase, as setting the value of the surface reaction term (Γ_s) is 2.5 ×10^{-4} in Eq. 3. A sensitivity simulation without considering

https://doi.org/10.5194/egusphere-2025-5093
Preprint. Discussion started: 28 October 2025

the surface hydrolysis (Γ_s is set to be 0 in Eq. 3), N_2O_5 uptake coefficient can be decreased to as low as 10^{-5} – 10^{-6} when the viscosity is higher than ~ 10^9 Pa s (Fig. S11), in which case N_2O_5 uptake is only limited by bulk diffusivity, and hence particle viscosity (Gržinić et al., 2015b; Song et al., 2025b).

By directly constraining temperature-dependent viscosity across a 30 K range and coupling it to global RH–temperature climatology, this study provides one of the first systematic experimental datasets for assessing OA phase behavior under realistic tropospheric conditions. These results highlight the necessity of incorporating temperature-sensitive viscosity parameterizations into next-generation air quality and climate models to more accurately predict particle lifetimes, reactivity, and cloud interactions.

https://doi.org/10.5194/egusphere-2025-5093
Preprint. Discussion started: 28 October 2025

Author Contributions

M.S. designed this study. A.U. and M.S. conducted viscosity experiments and analyzed the data. Y.L. calculated the reactive uptake of N_2O_5. A.U., Y.L., and M.S. wrote the manuscript.

Funding Sources

This work was supported by the National Research Foundation of Korea (NRF) grant funded by the Korea government (MSIT) (RS-2024-00335536), by Global - Learning & Academic research institution for Master's PhD students, and Postdocs (LAMP) Program of the NRF grant funded by the Ministry of Education (No. RS-2024-00443714), and by National Natural Science Foundation of China for funding (Nos. 42330605 and 42475124).

Notes

The authors declare no competing financial interest.

Acknowledgment

We thank Gyoung Hee Go for technical support.

https://doi.org/10.5194/egusphere-2025-5093
Preprint. Discussion started: 28 October 2025

References

Abbatt, J. P. D., Lee, A. K. Y., and Thornton, J. A.: Quantifying trace gas uptake to tropospheric aerosol: recent advances and remaining challenges, Chemical Society reviews, 41, 6555–6581, 10.1039/c2cs35052a, 2012.

Ammann, M., Cox, R. A., Crowley, J. N., Jenkin, M. E., Mellouki, A., Rossi, M. J., Troe, J., and Wallington, T. J.: Evaluated kinetic and photochemical data for atmospheric chemistry: Volume VI - heterogeneous reactions with liquid substrates, Atmospheric Chemistry and Physics, 13, 8045–8228, 10.5194/acp-13-8045-2013, 2013.

Angell, C.: Relaxation in liquids, polymers and plastic crystals—strong/fragile patterns and problems, Journal of Non-Crystalline Solids, 131, 13–31, 1991.

Bateman, A. P., Bertram, A. K., and Martin, S. T.: Hygroscopic influence on the semisolid-to-liquid transition of secondary organic materials, The journal of physical chemistry. A, 119, 4386–4395, 10.1021/jp508521c, 2014.

Champion, W. M., Rothfuss, N. E., Petters, M. D., and Grieshop, A. P.: Volatility and Viscosity Are Correlated in Terpene Secondary Organic Aerosol Formed in a Flow Reactor, Environmental Science & Technology Letters, 6, 513–519, 10.1021/acs.estlett.9b00412, 2019.

DeRieux, W.-S. W., Li, Y., Lin, P., Laskin, J., Laskin, A., Bertram, A. K., Nizkorodov, S. A., and Shiraiwa, M.: Predicting the glass transition temperature and viscosity of secondary organic material using molecular composition, Atmospheric Chemistry and Physics, 18, 6331–6351, 10.5194/acp-18-6331-2018, 2018.

Gerrebos, N. G. A., Zaks, J., Gregson, F. K. A., Walton-Raaby, M., Meeres, H., Zigg, I., Zandberg, W. F., and Bertram, A. K.: High Viscosity and Two Phases Observed over a Range of Relative Humidities in Biomass Burning Organic Aerosol from Canadian Wildfires, Environmental Science & Technology, 58, 21716–21728, 10.1021/acs.est.4c09148, 2024.

Grayson, J. W., Song, M., Sellier, M., and Bertram, A. K.: Validation of the poke-flow technique combined with simulations of fluid flow for determining viscosities in samples with small volumes and high viscosities, Atmospheric Measurement Techniques, 8, 2463–2472, 10.5194/amt-8-2463-2015, 2015.

https://doi.org/10.5194/egusphere-2025-5093
Preprint. Discussion started: 28 October 2025

Grayson, J. W., Zhang, Y., Mutzel, A., Renbaum-Wolff, L., Böge, O., Kamal, S., Herrmann, H., Martin, S. T., and Bertram, A. K.: Effect of varying experimental conditions on the viscosity of α -pinene derived secondary organic material, Atmospheric Chemistry and Physics, 16, 6027–6040, 10.5194/acp-16-6027-2016, 2016.

Grayson, J. W., Evoy, E., Song, M., Chu, Y., Maclean, A. M., Nguyen, A., Upshur, M. A., Ebrahimi, M., Chan, C. K., Geiger, F. M., Thomson, R. J., and Bertram, A. K.: The effect of hydroxyl functional groups and molar mass on the viscosity of non-crystalline organic and organic–water particles, Atmospheric Chemistry and Physics, 17, 8509–8524, 10.5194/acp-17-8509-2017, 2017.

Gregson, F. K. A., Gerrebos, N. G. A., Schervish, M., Nikkho, S., Schnitzler, E. G., Schwartz, C., Carlsten, C., Abbatt, J. P. D., Kamal, S., Shiraiwa, M., and Bertram, A. K.: Phase Behavior and Viscosity in Biomass Burning Organic Aerosol and Climatic Impacts, Environmental Science & Technology, 57, 14548–14557, 10.1021/acs.est.3c03231, 2023.

Gržinić, G., Bartels-Rausch, T., Berkemeier, T., Türler, A., and Ammann, M.: Viscosity controls humidity dependence of N2O5 uptake to citric acid aerosol, Atmospheric Chemistry and Physics, 15, 13615–13625, 10.5194/acp-15-13615-2015, 2015a.

Gržinić, G., Bartels-Rausch, T., Berkemeier, T., Türler, A., and Ammann, M.: Viscosity controls humidity dependence of N₂O₅ uptake to citric acid aerosol, Atmos. Chem. Phys., 15, 13615–13625, 10.5194/acp-15-13615-2015, 2015b.

Hallquist, M., Stewart, D., Stephenson, S. K., and Cox, R. A.: Hydrolysis of N2O5 on sub-micron sulfate aerosols, Physical Chemistry Chemical Physics, 5, 3453–3463, 10.1039/b301827j, 2003.

Jeong, R., Lilek, J., Zuend, A., Xu, R., Chan, M. N., Kim, D., Moon, H. G., and Song, M.: Viscosity and physical state of sucrose mixed with ammonium sulfate droplets, Atmospheric Chemistry and Physics, 22, 8805–8817, 10.5194/acp-22-8805-2022, 2022.

https://doi.org/10.5194/egusphere-2025-5093
Preprint. Discussion started: 28 October 2025

Kasparoglu, S., Li, Y., Shiraiwa, M., and Petters, M. D.: Toward closure between predicted and observed particle viscosity over a wide range of temperatures and relative humidity, Atmos. Chem. Phys., 21, 1127–1141, 10.5194/acp-21-1127-2021, 2021.

Kiland, K. J., Maclean, A. M., Kamal, S., and Bertram, A. K.: Diffusion of Organic Molecules as a Function of Temperature in a Sucrose Matrix (a Proxy for Secondary Organic Aerosol), The journal of physical chemistry letters, 10, 5902–5908, 10.1021/acs.jpclett.9b02182, 2019.

Kiland, K. J., Mahrt, F., Peng, L., Nikkho, S., Zaks, J., Crescenzo, G. V., and Bertram, A. K.: Viscosity, Glass Formation, and Mixing Times within Secondary Organic Aerosol from Biomass Burning Phenolics, ACS Earth and Space Chemistry, 7, 1388–1400, 10.1021/acsearthspacechem.3c00039, 2023.

Knopf, D. A., Alpert, P. A., and Wang, B.: The Role of Organic Aerosol in Atmospheric Ice Nucleation: A Review, ACS Earth and Space Chemistry, 2, 168–202, 10.1021/acsearthspacechem.7b00120, 2018.

Koop, T., Bookhold, J., Shiraiwa, M., and Pöschl, U.: Glass transition and phase state of organic compounds: dependency on molecular properties and implications for secondary organic aerosols in the atmosphere, Physical chemistry chemical physics : PCCP, 13, 19238–19255, 10.1039/c1cp22617g, 2011.

Kuwata, M. and Martin, S. T.: Phase of atmospheric secondary organic material affects its reactivity, Proc. Natl. Acad. Sci. U. S. A., 109, 17354–17359, 10.1073/pnas.1209071109, 2012.

Ladino, L. A., Zhou, S., Yakobi-Hancock, J. D., Aljawhary, D., and Abbatt, J.: Factors controlling the ice nucleating abilities of α-pinene SOA particles, Journal of Geophysical Research: Atmospheres, 119, 9041–9051, 10.1002/2014jd021578, 2014.

Li, Y., Day, D. A., Stark, H., Jimenez, J. L., and Shiraiwa, M.: Predictions of the glass transition temperature and viscosity of organic aerosols from volatility distributions, Atmospheric Chemistry and Physics, 20, 8103–8122, 10.5194/acp-20-8103-2020, 2020.

https://doi.org/10.5194/egusphere-2025-5093
Preprint. Discussion started: 28 October 2025

Lienhard, D. M., Huisman, A. J., Krieger, U. K., Rudich, Y., Marcolli, C., Luo, B. P., Bones, D. L., Reid, J. P., Lambe, A. T., Canagaratna, M. R., Davidovits, P., Onasch, T. B., Worsnop, D. R., Steimer, S. S., Koop, T., and Peter, T.: Viscous organic aerosol particles in the upper troposphere: diffusivity-controlled water uptake and ice nucleation?, Atmospheric Chemistry and Physics, 15, 13599–13613, 10.5194/acp-15-13599-2015, 2015.

Maclean, A. M., Smith, N. R., Li, Y., Huang, Y., Hettiyadura, A. P. S., Crescenzo, G. V., Shiraiwa, M., Laskin, A., Nizkorodov, S. A., and Bertram, A. K.: Humidity-Dependent Viscosity of Secondary Organic Aerosol from Ozonolysis of β-Caryophyllene: Measurements, Predictions, and Implications, ACS Earth and Space Chemistry, 5, 305–318, 10.1021/acsearthspacechem.0c00296, 2021a.

Maclean, A. M., Li, Y., Crescenzo, G. V., Smith, N. R., Karydis, V. A., Tsimpidi, A. P., Butenhoff, C. L., Faiola, C., Lelieveld, J., Nizkorodov, S. A., Shiraiwa, M., and Bertram, A. K.: Global Distribution of the Phase State and Mixing Times within Secondary Organic Aerosol Particles in the Troposphere Based on Room-Temperature Viscosity Measurements, ACS Earth and Space Chemistry, 5, 3458–3473, 10.1021/acsearthspacechem.1c00296, 2021b.

Marshall, F., Berkemeier, T., Shiraiwa, M., Nandy, L., Ohm, P., Dutcher, C. S., and Reid, J. P.: Influence of particle viscosity on mass transfer and heterogeneous ozonolysis kinetics in aqueous–sucrose–maleic acid aerosol, Physical chemistry chemical physics : PCCP, 20, 15560–15573, 10.1039/c8cp01666f, 2018.

Marshall, F. H., Miles, R. E. H., Song, Y.-C., Ohm, P. B., Power, R. M., Reid, J. P., and Dutcher, C. S.: Diffusion and reactivity in ultraviscous aerosol and the correlation with particle viscosity, Chemical Science, 7, 1298–1308, 10.1039/C5SC03223G, 2016.

Nikkho, S., Bai, B., Mahrt, F., Zaks, J., Peng, L., Kiland, K. J., Liu, P. F., and Bertram, A. K.: Secondary Organic Aerosol from Biomass Burning Phenolic Compounds and Nitrate Radicals can be Highly Viscous over a Wide Relative Humidity Range, Environmental Science & Technology, 58, 21702–21715, 10.1021/acs.est.4c06235, 2024.

https://doi.org/10.5194/egusphere-2025-5093
Preprint. Discussion started: 28 October 2025

Pandis, S. N., Harley, R. A., Cass, G. R., and Seinfeld, J. H.: Secondary organic aerosol formation and transport, Atmospheric Environment. Part A. General Topics, 26, 2269–2282, 10.1016/0960-1686(92)90358-r, 1992.

Pöschl, U.: Atmospheric aerosols:: Composition, transformation, climate and health effects, Angew Chem Int Edit, 44, 7520–7540, 10.1002/anie.200501122, 2005.

Power, R. M., Simpson, S. H., Reid, J. P., and Hudson, A. J.: The transition from liquid to solid-like behaviour in ultrahigh viscosity aerosol particles, Chemical Science, 4, 2597–2604, 10.1039/c3sc50682g, 2013.

Reid, J. P., Bertram, A. K., Topping, D., Laskin, A., Martin, S. T., Petters, M. D., Pope, F. D., and Rovelli, G.: The viscosity of atmospherically relevant organic particles, Nature communications, 9, 956–956, 10.1038/s41467-018-03027-z, 2018.

Renbaum-Wolff, L., Grayson, J., and Bertram, A.: New methodology for measuring viscosities in small volumes characteristic of environmental chamber particle samples, Atmospheric Chemistry and Physics, 13, 791–802, 2013a.

Renbaum-Wolff, L., Grayson, J. W., and Bertram, A. K.: Technical Note: New methodology for measuring viscosities in small volumes characteristic of environmental chamber particle samples, Atmospheric Chemistry and Physics, 13, 791–802, 10.5194/acp-13-791-2013, 2013b.

Renbaum-Wolff, L., Grayson, J. W., Bateman, A. P., Kuwata, M., Sellier, M., Murray, B. J., Shilling, J. E., Martin, S. T., and Bertram, A. K.: Viscosity of α-pinene secondary organic material and implications for particle growth and reactivity, Proc. Natl. Acad. Sci. U. S. A., 110, 8014–8019, 10.1073/pnas.1219548110, 2013c.

Rothfuss, N. E. and Petters, M. D.: Influence of Functional Groups on the Viscosity of Organic Aerosol, Environmental Science & Technology, 51, 271–279, 10.1021/acs.est.6b04478, 2017a.

Rothfuss, N. E. and Petters, M. D.: Characterization of the temperature and humidity-dependent phase diagram of amorphous nanoscale organic aerosols, Physical chemistry chemical physics : PCCP, 19, 6532–6545, 10.1039/c6cp08593h, 2017b.

https://doi.org/10.5194/egusphere-2025-5093
Preprint. Discussion started: 28 October 2025

Saukko, E., Lambe, A. T., Massoli, P., Koop, T., Wright, J. P., Croasdale, D. R., Pedernera, D. A., Onasch, T. B., Laaksonen, A., Davidovits, P., Worsnop, D. R., and Virtanen, A.: Humidity-dependent phase state of SOA particles from biogenic and anthropogenic precursors, Atmospheric Chemistry and Physics, 12, 7517–7529, 10.5194/acp-12-7517-2012, 2012.

Sellier, M., Grayson, J. W., Renbaum-Wolff, L., Song, M., and Bertram, A. K.: Estimating the viscosity of a highly viscous liquid droplet through the relaxation time of a dry spot, Journal of Rheology, 59, 733–750, 10.1122/1.4917240, 2015.

Shiraiwa, M. and Seinfeld, J. H.: Equilibration timescale of atmospheric secondary organic aerosol partitioning, Geophysical Research Letters, 39, NA–NA, 10.1029/2012gl054008, 2012.

Shiraiwa, M., Ammann, M., Koop, T., and Pöschl, U.: Gas uptake and chemical aging of semisolid organic aerosol particles, Proc. Natl. Acad. Sci. U. S. A., 108, 11003–11008, 10.1073/pnas.1103045108, 2011.

Shiraiwa, M., Yee, L. D., Schilling, K. A., Loza, C. L., Craven, J. S., Zuend, A., Ziemann, P. J., and Seinfeld, J. H.: Size distribution dynamics reveal particle-phase chemistry in organic aerosol formation, Proc. Natl. Acad. Sci. U. S. A., 110, 11746–11750, 10.1073/pnas.1307501110, 2013.

Shiraiwa, M., Li, Y., Tsimpidi, A. P., Karydis, V. A., Berkemeier, T., Pandis, S. N., Lelieveld, J., Koop, T., and Pöschl, U.: Global distribution of particle phase state in atmospheric secondary organic aerosols, Nature communications, 8, 15002–15002, 10.1038/ncomms15002, 2017.

Song, M., Liu, P., Hanna, S. J., Li, Y. J., Martin, S. T., and Bertram, A. K.: Relative humidity-dependent viscosities of isoprene-derived secondary organic material and atmospheric implications for isoprene-dominant forests, Atmospheric Chemistry and Physics, 15, 5145–5159, 10.5194/acp-15-5145-2015, 2015a.

Song, M., Liu, P. F., Hanna, S. J., Li, Y. J., Martin, S. T., and Bertram, A. K.: Relative humidity-dependent viscosities of isoprene-derived secondary organic material and atmospheric implications for isoprene-dominant forests, Atmos. Chem. Phys., 15, 5145–5159, 10.5194/acp-15-5145-2015, 2015b.

https://doi.org/10.5194/egusphere-2025-5093
Preprint. Discussion started: 28 October 2025

Song, M., Liu, P., Hanna, S. J., Zaveri, R. A., Potter, K. J., You, Y., Martin, S. T., and Bertram, A. K.: Relative humidity-dependent viscosity of secondary organic material from toluene photo-oxidation and possible implications for organic particulate matter over megacities, Atmospheric Chemistry and Physics, 16, 8817–8830, 10.5194/acp-16-8817-2016, 2016a.

Song, M., Li, Y., Seong, C., Yang, H., Jang, K.-S., Wu, Z., Lee, J. Y., Matsuki, A., and Ahn, J.: Direct Observation of Liquid–Liquid Phase Separation and Core–Shell Morphology of PM2.5 Collected from Three Northeast Asian Cities and Implications for N2O5 Hydrolysis, ACS ES&T Air, 2, 1079–1088, 10.1021/acsestair.5c00043, 2025a.

Song, M., Li, Y., Seong, C., Yang, H., Jang, K.-S., Wu, Z., Lee, J. Y., Matsuki, A., and Ahn, J.: Direct Observation of Liquid–Liquid Phase Separation and Core–Shell Morphology of PM2.5 Collected from Three Northeast Asian Cities and Implications for N2O5 Hydrolysis, ACS ES&T Air, 10.1021/acsestair.5c00043, 2025b.

Song, M., Maclean, A. M., Huang, Y., Smith, N. R., Blair, S. L., Laskin, J., Laskin, A., DeRieux, W.-S. W., Li, Y., Shiraiwa, M., Nizkorodov, S. A., and Bertram, A. K.: Liquid-liquid phase separation and viscosity within secondary organic aerosol generated from diesel fuel vapors, Atmospheric Chemistry and Physics, 19, 12515–12529, 10.5194/acp-19-12515-2019, 2019a.

Song, M., Maclean, A. M., Huang, Y., Smith, N. R., Blair, S. L., Laskin, J., Laskin, A., DeRieux, W. S. W., Li, Y., Shiraiwa, M., Nizkorodov, S. A., and Bertram, A. K.: Liquid–liquid phase separation and viscosity within secondary organic aerosol generated from diesel fuel vapors, Atmos. Chem. Phys., 19, 12515–12529, 10.5194/acp-19-12515-2019, 2019b.

Song, M., Jeong, R., Kim, D., Qiu, Y., Meng, X., Wu, Z., Zuend, A., Ha, Y., Kim, C., Kim, H., Gaikwad, S., Jang, K.-S., Lee, J. Y., and Ahn, J.: Comparison of Phase States of PM2.5 over Megacities, Seoul and Beijing, and Their Implications on Particle Size Distribution, Environmental science & technology, 56, 17581–17590, 10.1021/acs.est.2c06377, 2022.

https://doi.org/10.5194/egusphere-2025-5093
Preprint. Discussion started: 28 October 2025

Song, Y.-C., Lilek, J., Lee, J. B., Chan, M. N., Wu, Z., Zuend, A., and Song, M.: Viscosity and phase state of aerosol particles consisting of sucrose mixed with inorganic salts, Atmospheric Chemistry and Physics, 21, 10215–10228, 10.5194/acp-21-10215-2021, 2021a.

Song, Y. C., Lilek, J., Lee, J. B., Chan, M. N., Wu, Z. J., Zuend, A., and Song, M. J.: Viscosity and phase state of aerosol particles consisting of sucrose mixed with inorganic salts, Atmospheric Chemistry and Physics, 21, 10215–10228, 10.5194/acp-21-10215-2021, 2021b.

Song, Y. C., Haddrell, A. E., Bzdek, B. R., Reid, J. P., Bannan, T. J., Topping, D., Percival, C. J., and Cai, C.: Measurements and Predictions of Binary Component Aerosol Particle Viscosity, The journal of physical chemistry. A, 120, 8123–8137, 10.1021/acs.jpca.6b07835, 2016b.

Wagner, N. L., Riedel, T. P., Young, C. J., Bahreini, R., Brock, C. A., Dubé, W. P., Kim, S., Middlebrook, A. M., Öztürk, F., Roberts, J. M., Russo, R., Sive, B., Swarthout, R., Thornton, J. A., VandenBoer, T. C., Zhou, Y., and Brown, S. S.: N2O5 uptake coefficients and nocturnal NO2 removal rates determined from ambient wintertime measurements, Journal of Geophysical Research: Atmospheres, 118, 9331–9350, 10.1002/jgrd.50653, 2013.

You, Y., Renbaum-Wolff, L., Carreras-Sospedra, M., Hanna, S. J., Hiranuma, N., Kamal, S., Smith, M. L., Zhang, X., Weber, R. J., Shilling, J. E., Dabdub, D., Martin, S. T., and Bertram, A. K.: Images reveal that atmospheric particles can undergo liquid–liquid phase separations, Proceedings of the National Academy of Sciences, 109, 13188–13193, 10.1073/pnas.1206414109, 2012.

Zaveri, R. A., Shilling, J. E., Zelenyuk, A., Liu, J., Bell, D. M., D'Ambro, E. L., Gaston, C. J., Thornton, J. A., Laskin, A., Lin, P., Wilson, J. M., Easter, R. C., Wang, J., Bertram, A. K., Martin, S. T., Seinfeld, J. H., and Worsnop, D. R.: Growth Kinetics and Size Distribution Dynamics of Viscous Secondary Organic Aerosol, Environmental science & technology, 52, 1191–1199, 10.1021/acs.est.7b04623, 2018.

https://doi.org/10.5194/egusphere-2025-5093
Preprint. Discussion started: 28 October 2025

Zhang, T., Zuo, P., Chen, Y., Liu, T., Zeng, L., Lin, W., and Ye, C.: Measurement report: Variations and environmental impacts of atmospheric N2O5 concentrations in urban Beijing during the 2022 Winter Olympics, EGUsphere, 2025, 1–23, 10.5194/egusphere-2025-2210, 2025.

Zhou, S., Shiraiwa, M., McWhinney, R. D., Pöschl, U., and Abbatt, J. P. D.: Kinetic limitations in gas-particle reactions arising from slow diffusion in secondary organic aerosol, Faraday Discuss., 165, 391–406, 10.1039/c3fd00030c, 2013.

Zobrist, B., Soonsin, V., Luo, B. P., Krieger, U. K., Marcolli, C., Peter, T., and Koop, T.: Ultra-slow water diffusion in aqueous sucrose glasses, Physical chemistry chemical physics : PCCP, 13, 3514–3526, 10.1039/c0cp01273d, 2011.